Korean J. Chem. Eng., 39(11), 2983-2990 (2022)
DOI: 10.1007/s11814-022-1215-z

pISSN: 0256-1115
eISSN: 1975-7220

The improvement effect of surfactants on hydrogenation at condition containing water for Cu/SiO_2 catalysts

Zheng Chen*,†, Xueying Zhao*, Shuwei Wei*, Dengfeng Wang*, Xuelan Zhang*, and Jianfeng Shan*,,†**

*College of Chemistry, Chemical Engineering and Materials Science, Zaozhuang University, Zaozhuang 277160, Shandong, China
**College of Chemistry and Chemical Engineering, Xinyang Normal University, Xinyang 464000, China
(*Received 16 February 2022 • Revised 21 May 2022 • Accepted 25 June 2022*)

Abstract−In the industrial production, water exists inevitably into feed stocks in the form of impurity, and it can produce a negative effect in the hydrogenation reaction due to the preferential adsorption of water on active sites. Here, the surfactants (polyvinylpyrrolidone, poloxamer, polyethylene glycol and hexadecyl trimethyl ammonium bromide) are used to improve physicochemical property of Cu/SiO_2 catalysts, so that Cu/SiO_2 catalysts had a good hydrogenation performance at condition containing water. The appropriate addition amount of surfactants in the catalyst preparation process effectively hindered the agglomeration of copper species by steric configuration and repulsion effect between Cu^{2+} and positive ionizable, which brought about high copper dispersion and small particle size. Meanwhile, the decomposition of surfactants produced many pores during calcination, resulting in the increased of specific surface area and average pore diameter. These advantages provided more chances for reactants to touch active sites due to spatial restriction and the increase of the number of active sites, so that the negative effects of water can be counteracted. The conversion of Cu/SiO_2 catalysts, that the surfactants was added in the catalyst preparation process, increased 60% to 200% at reaction condition containing water.

Keywords: Hydrogenation, Surfactant, Copper, Water, Ethanol

INTRODUCTION

Ethanol, as a kind of renewable resources, is not only a basic organic chemical raw material and an important solvent, but also environmentally friendly clean fuel and oil quality improver [1-3]. Although ethanol can be produced by the fermentation of grain and biomass, the hydrogenation of coal and biomass to ethanol have huge advantages in the long run, because that it meets clean and efficient use of resources and environmental protection [1-3]. At present, two kinds of technology, that the direct and indirect utilization of biomass and coal, are used to produce ethanol. Thereinto, the indirect method, that acetates are first prepared from syngas and then hydrogenated to ethanol, is adopted extensively due to the mild reaction conditions, high one-way conversion and technical maturity. Meanwhile, copper-based catalysts were usually used to catalyse acetates hydrogenation to ethanol due to its selective hydrogenation for carbonyl group and inactive hydrogenolysis for carbon-carbon bonds [4,5].

However, in the process of the indirect utilization of biomass and coal, water is often contained in acetates in the form of impurity. And acetates can be obtained as byproduct from chemical production, which also contain water. Water is easy to case the problems for copper-based catalysts in the gas-phase hydrogenation reaction, such as particle growth, life shortening, the reduction of conversion [6,7]. However, water removal will increase energy consumption and equipment investment, which are not conducive to energy conservation and emission reduction. Therefore, the development of high efficiency water-tolerant copper-based catalysts is necessary. The previous work had confirmed that the preferential adsorption of water onto Cu^+ sites was the main reason of deactivation for ethyl acetate hydrogenation, and the next was particle growth for Cu/SiO_2 catalyst at condition containing water [7]. And the increase of the amount of active sites is beneficial to remedy the negative effect due to the preferential adsorption of water [6]. Therefore, it was feasible to improve the hydrogenation water-tolerant of Cu/SiO_2 catalyst by the increase of copper dispersion. Meanwhile, the studies had indicated spatial restriction had an important effect on the diffusion, adsorption and reaction processes in the catalytic reaction, which could limit the growth of catalyst particles and improve the catalytic activity [8-11].

The addition of surfactants into the preparation process can effectively promote the dispersion of active component, and the pore structure can also be produced during calcination. Wang et al. [12] used polyvinylpyrrolidone as an assistant to prepare MnO_2-CoO_X catalysts and found Mn-Co-0.2-PVP catalyst had high NO conversion and good H_2O and SO_2 resistance. The small-sized SAPO-34 were synthesized by the addition of Pluronic F127 nonionic surfactant (growth inhibitor), which had good stability for the reaction of methanol to olefins [13]. The result proved that the Pluronic F127 was responsible for Si dispersion and the crystalline size in the gel. The polyethylene glycol was used to increase poriness and amend surface functional groups of the Cu-Zn catalysts for meth-

†To whom correspondence should be addressed.
E-mail: chenzhengtt@163.com, shan_jianfeng@foxmail.com

anol synthesis [14[. Mao et al. [15] synthesized a sequence of CuO/ZnO/ZrO_2 catalysts, which were evaluated by the hydrogenation of CO_2 to methanol. The excellent hydrogenation performance was attributed to high element dispersion, close interfacial contact between Cu species and ZrO_2 and/or ZnO and porous structure with a large aperture due to the addition of cetyltrimethyl ammonium bromide. Moreover, the surfactants, sodium dodecyl benzene sulfonate, triblock copolymer P123, sodium dodecyl sulfate and so on, for instance, were used to change the physicochemical property of catalysts, so that catalytic performance was improved [16-21].

In this paper, polyvinylpyrrolidone, poloxamer, polyethylene glycol and hexadecyl trimethyl ammonium bromide are added into the preparation process to study the influence of surfactants on physicochemical property of Cu/SiO_2 catalysts, contributing to an excellent hydrogenation performance at condition containing water. The catalytic performances are correlated with characterization results to show the improvement of copper dispersion and pore structure of Cu/SiO_2 catalysts influence on water-tolerant performance.

EXPERIMENTAL

1. Material

The analytically pure grade of Copper(ii) nitrate hydrate, tetraethyl orthosilicate, ethyl alcohol absolute, ammonium bicarbonate, polyvinylpyrrolidone (PVP), poloxamer (F127), polyethylene glycol (PEG-2000) and hexadecyl trimethyl ammonium bromide (CTAB) were bought from Sinopharm Chemical Reagent Co., Ltd and directly used.

2. The Preparation of Catalyst

The catalysts were synthesized by precipitation method and used ammonium bicarbonate as precipitant. The synthesized catalysts were tagged as Cu/SiO_2, Cu/SiO_2-P (PVP), Cu/SiO_2-PG (PEG-2000), Cu/SiO_2-F (F127) and Cu/SiO_2-C (CTAB) on the basis of different surfactants. And the nominal copper loading of the catalysts was 25%.

For Cu/SiO_2 catalyst, copper(ii) nitrate hydrate (6.05 g) was added into mixed solution (deionized water/ethanol=50 ml/50 ml). For other catalysts, except for copper nitrate hydrate, 0.5 g of PVP, PEG-2000, F127 and CTAB were added into mixed solution, respectively. Then tetraethyl orthosilicate (53.72 g) and 200 ml NH_4HCO_3 aqueous solution were added into above mixed solution in turn. Thereafter, mixed solution was stirred at 90 °C for 3 h. And then the mixed solution was aged at room temperature for 12 h. After the process of centrifugation and drying, the catalyst precursors were obtained.

Moreover, in order to analyse the effect of surfactant amount, 1 g and 3 g of F127 were also added into mixed solution to prepare Cu/SiO_2-F1 and Cu/SiO_2-F3 catalysts.

Finally, the muffle furnace was used to calcine catalyst precursors at 400 °C for 4 h and then pelletized, shed and sieved to 40-60 meshes.

3. Hydrogenation Reaction

The fixed bed reactor was used to evaluate catalytic properties of Cu/SiO_2 catalysts. The Brooks 5850E mass flow controller (MFC) was used to control H_2 flow. During the whole evaluation period, the back pressure regulator was used to maintain reaction pressure at 2.5 MPa. At first, in-situ reduction was performed by the used of H_2 (30 ml min^{-1}) at 300 °C for 4 h. Then, the temperature was increased to reaction temperature by 1 °C·min^{-1}, when temperature decreased from reduction temperature to room temperature. The ethyl acetate containing 5 wt% water was injected, and mixed with H_2 after vaporizing by a preheater. The gas chromatography (Shimadzu GC-14C) was used to analyse liquid products, which was collected by a 5 °C cooling trap. The gas chromatographs (Shanghai Haixin GC-950) was used to online analyse gas products.

The detail information of characterization methods could be found from the supporting materials.

RESULT AND DISCUSSION

In order to explore the effect of surfactants on the phases and crystal texture of prepared catalysts, XRD of catalyst precursors was performed (Fig. 1(a)). From Fig. 1(a), just a broad peak is observed at 22°, which is assigned to the (1 0 1) crystal face of silica (PDF#39-1425). And no obvious peaks relating to copper is found, showing the high dispersion or amorphous states of the copper species. However, it is clear that peak intensity of SiO_2 decreases due to the addition of surfactants, suggesting that the particle sizes of SiO_2 support become small. Furthermore, Fig. 1(b) showed XRD of the prepared catalysts after calcination. The similar phenomena of Fig. 1(a) is observed for Cu/SiO_2 catalysts after calcination, suggesting copper species are also high dispersion. However, the XRD pattern of Cu/SiO_2-P catalyst shows a peak corresponding to the (−1 1 1) crystal face of CuO at 35.5° (PDF#45-0937), indicating the crystallinity of CuO is higher than other catalysts. Therefore, it is found that the addition of surfactants have an obvious effect on crystal structure of Cu/SiO_2 catalysts.

The catalytic activity of Cu/SiO_2 catalysts was related with the average volume-surface diameter (d_{Cu}), specific surface area (S_{Cu}) and dispersion (D_{Cu}) of metal copper after reduction. In order to analyse the effect of the addition of surfactants on copper species, N_2O titration was performed and the results were showed in Fig. 2 and Table 1. From Table 1, it is found that the dispersion of metal copper increases due to the addition of surfactants, bringing about the higher S_{Cu} and smaller d_{Cu}. This may be because that the addi-

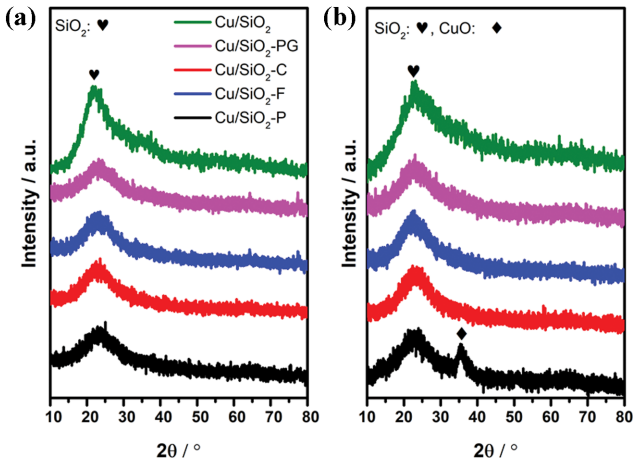

Fig. 1. XRD pattern of the prepared catalysts before (a) and after (b) calcination.

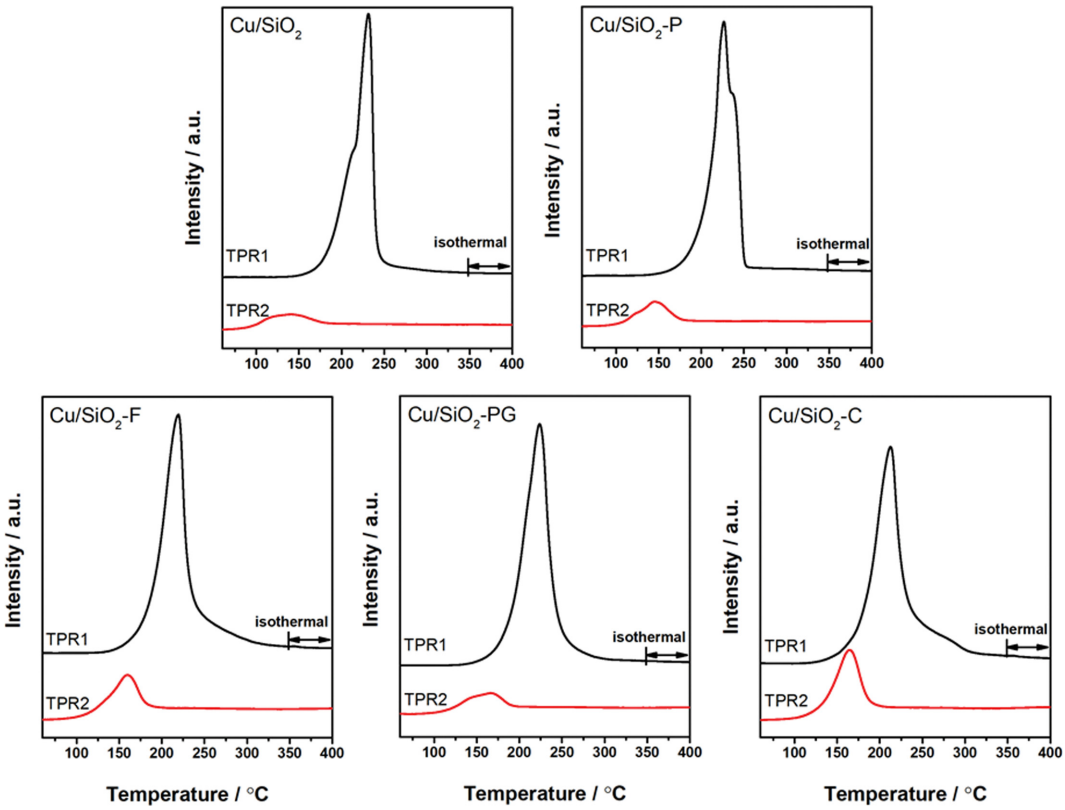

Fig. 2. TPR pattern of the prepared catalysts before and after N_2O oxidation at 50 °C.

Table 1. Textural properties of Cu/SiO_2 catalysts

Catalysts	S_{Cu} ($m_{Cu}^2 \cdot g_{Cu}^{-1}$)	D_{Cu} (%)	d_{Cu} (nm)	S_{BET} ($m^2 \cdot g^{-1}$)	V_p ($cm^3 \cdot g^{-1}$)	D_a (nm)
Cu/SiO_2	135.0	20.0	5.0	40.7	0.14	7.2
Cu/SiO_2-PG	152.7	22.5	4.4	116.7	0.47	16.0
Cu/SiO_2-P	170.0	25.1	4.0	192.4	0.06	11.3
Cu/SiO_2-F	234.6	34.7	2.9	121.4	0.43	14.0
Cu/SiO_2-C	309.8	45.8	2.2	253.7	0.71	11.3

S_{Cu}=1353 Y/X, D_{Cu}=2 Y/X, d_{Cu}=0.5 X/Y. X=the area of TPR1 peak and Y=the area of TPR2 peak which determined by N_2O titration [22,23].

tion of surfactants hinders the agglomeration of $Cu(OH)_2$ by steric configuration in the preparation process, so that copper species can evenly distributed on support surface. Specifically, the copper dispersion of Cu/SiO_2-C catalyst (45.8%) increases two times in comparison with that of Cu/SiO_2 catalyst (20%). The repulsion effect between Cu^{2+} and positive ionizable for CTAB (cationic surfactant), was also responsible for high copper dispersion and small particle size.

The addition of surfactants not only has a great effect on the copper species, but also SiO_2 support. Therefore, N_2 adsorption-desorption was performed to exhibit the change of specific surface area (S_{BET}), cumulative volume (V_p) and average pore diameter (D_a) of Cu/SiO_2 catalysts (Fig. 3), and the relative results were also shown in Table 1. The Fig. 3(a) shows the adsorption-desorption isotherms of Cu/SiO_2 catalysts. It is clear that Cu/SiO_2 catalyst is of type III and the hysteresis loops belongs to H3 type with aggregates of plate-like particles causing slit-shaped pores, on the basis of IUPAC

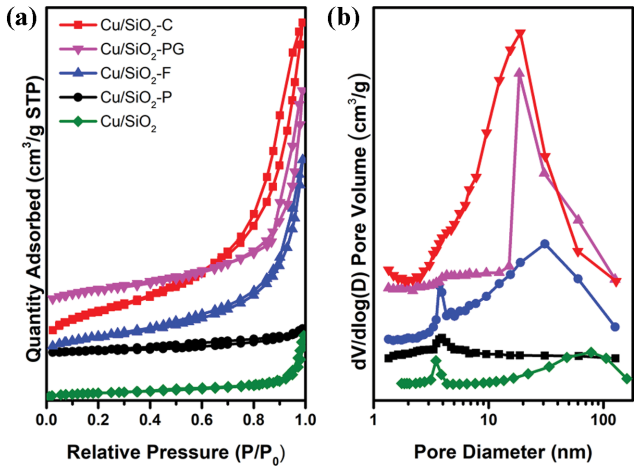

Fig. 3. (a) N_2 adsorption-desorption isotherms and (b) BJH desorption pore size distribution for all catalysts.

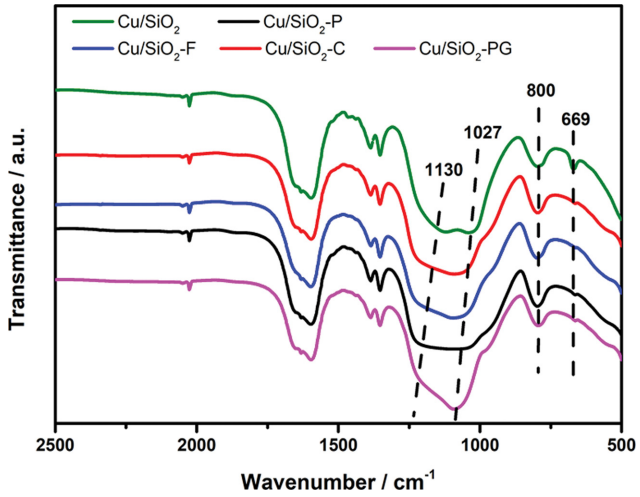

Fig. 4. FT-IR of the prepared catalysts.

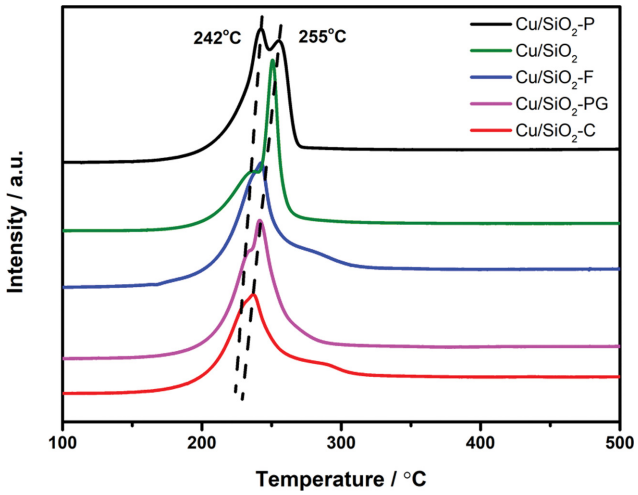

Fig. 5. H_2-temperature-programmed reduction pattern of the prepared catalysts.

Classification [24,25]. This conclusion is in well agreement with the result of TEM (Fig. 6), which shows the lamellar structure. The Fig. 3(b) shows BJH desorption pore size distribution, which indicates that the addition of surfactants leads to the production of mesoporous and concentration of pore size distribution. From Table 1, the S_{BET} of Cu/SiO_2 catalysts increase three to six times because of the addition of surfactants. Specifically, the S_{BET} of Cu/SiO_2-C catalyst increases six times (253.7 $m^2 \cdot g^{-1}$) in comparison with Cu/SiO_2 catalyst (40.7 $m^2 \cdot g^{-1}$). It may because lamellar structure is crumbled

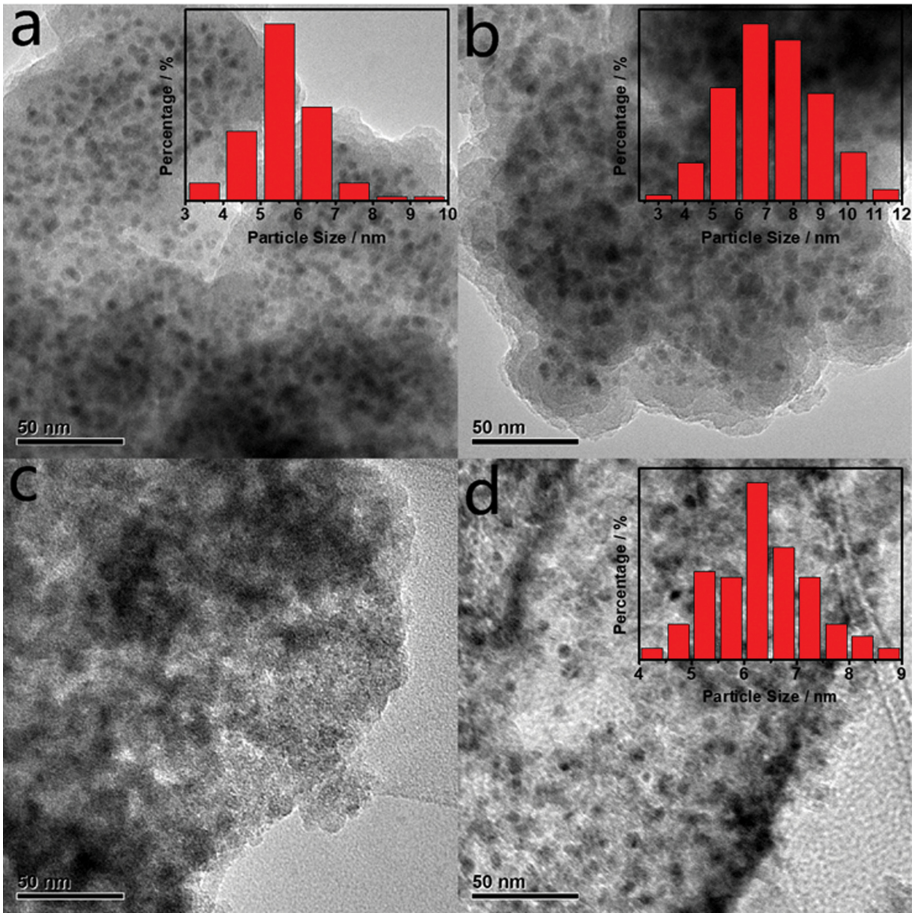

Fig. 6. The TEM images of the Cu/SiO_2 catalyst (a), (b) and Cu/SiO_2-F (c), (d) catalyst before (a), (c) and after (b), (d) reaction.

Table 2. Binding energies of Cu $2p_{3/2}$ for prepared catalysts

Sample	Cu/SiO_2	Cu/SiO_2-C	Cu/SiO_2-F	Cu/SiO_2-PG	Cu/SiO_2-P
Cu_1^{2+} (eV)	933.3	933.6	933.2	933.2	933.0
Cu_2^{2+} (eV)	935.7	935.8	935.7	935.6	935.3
$Cu_1^{2+}/(Cu_1^{2+}+Cu_2^{2+})^a$ (%)	26.6	43.0	28.7	14.4	26.2

[a]Percent of relative amount of the copper species evaluated by XPS

due to the pyrolysis of surfactants in the calcination. From Table 1, it is also found that the V_p increases three to five times, except for Cu/SiO_2-P catalyst, which are 0.14, 0.47, 0.43, and 0.71 $cm^3 \cdot g^{-1}$ for Cu/SiO_2, Cu/SiO_2-PG, Cu/SiO_2-F and Cu/SiO_2-C, respectively. The cumulative volume (0.06 $cm^3 \cdot g^{-1}$) of Cu/SiO_2-P catalyst decreases two times in comparison with Cu/SiO_2 catalyst (0.14 $cm^3 \cdot g^{-1}$).

Fig. 4 shows the FT-IR of Cu/SiO_2 catalysts. The ν_{SiO} asymmetric stretching and asymmetric band of silica can be observed from 800 cm^{-1} and 1,130 cm^{-1} [26-28]. And the δ_{OH} band and the ν_{SiO} of copper phyllosilicate can be found from 669 cm^{-1} and 1,027 cm^{-1} [26-28]. Furthermore, the addition of surfactants leads to decrease the intensity of absorption peak at 669 cm^{-1}, suggesting the content of copper phyllosilicate reduced. This is because the addition of surfactants hindered the interaction of Si and Cu in the preparation process. However, the interaction of Si-O becomes strong due to the observation of the blue-shift at absorption peaks of 1,027 cm^{-1} and 1,130 cm^{-1}. Therefore, the addition of surfactants hinder the interaction Cu and Si, but enhanced the interaction of Si-O.

Fig. 5 shows the result of H_2-temperature-programmed reduction and two reduction peaks can be observed for all catalysts. These peaks are assigned to the reduction of CuO to Cu_2O (242 °C) and Cu_2O to Cu (255 °C). From Fig. 5, except for Cu/SiO_2-P, the reduction temperatures decrease due to the addition of surfactants. However, the reduction temperature of Cu/SiO_2-P catalyst increase which may be because that the high crystallinity of CuO.

The TEM images of the catalysts before and after reaction are shown in Fig. 6. From Fig. 6(a), it is observed that the copper species are highly dispersed onto multilayer lamellar structure of silica support and the particle sizes are mainly concentrated in the range of 4-8 nm. Although copper species grow up (5-10 nm) after reaction, they also have a relatively high dispersion for Cu/SiO_2 catalyst, as shown in Fig. 6(b). For Cu/SiO_2-F catalyst, the big lamellar structure is damaged by calcination to form small block, so that more active sites can be exposed (Fig. 6(c)). And there is no particle observed from Fig. 6(c). After reaction, copper species are also uniform distributed on SiO_2 with the particle size range of 5-8 nm, as shown in Fig. 6(d). Furthermore, it is referred that the copper species are confined in SiO_2 interlayer for Cu/SiO_2 catalyst (Fig. 6(a)), so that its anti-sintering ability is good. However, the anti-sintering ability has a declining trend for Cu/SiO_2-F catalyst, because that none particle is observed before reaction but 5-8 nm after reaction.

The XPS of the prepared catalysts were performed and the relative results were showed in Table 2 and Fig. S1. It is clear that two peaks at around 935 eV and 955 eV are observed from Fig. S1, and all catalysts show the satellite peaks of 2p→3d at around 943 eV and 964 eV, suggesting the existence of Cu^{2+} [29-31]. Furthermore, the binding energies of Cu $2p_{3/2}$ contain two peaks, which is deconvoluted into two symmetric peaks (Fig. S1), indicating that two types of Cu^{2+} species exist in the prepared catalysts. The published work had confirmed that the binding energy at around 933.5 eV was related with CuO species; and the peak at around 935.0 eV was assigned to Cu^{2+} with strong interaction with SiO_2 [32,33]. Meanwhile, $Cu_1^{2+}/(Cu_1^{2+}+Cu_2^{2+})$ is calculated by relative integral area to

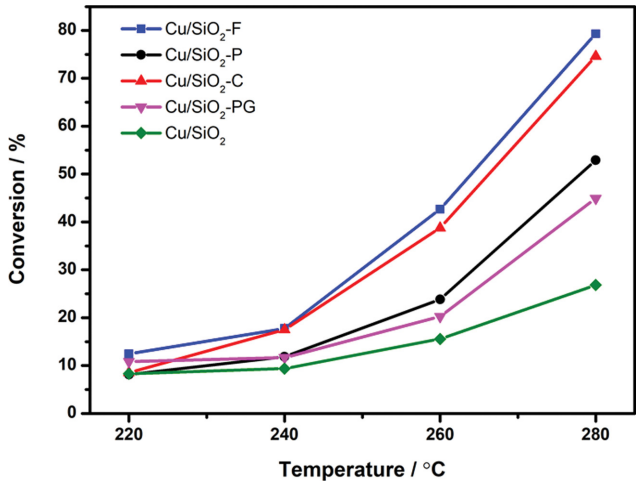

Fig. 7. The conversion of ethyl acetate for the prepared catalysts at condition: T=220, 240, 260 and 280 °C; LHSV of ethyl acetate= 1 h^{-1}; n(H_2)/n(ethyl acetate with 5 wt% water)=40 (molar ration) and P=2.5 MPa.

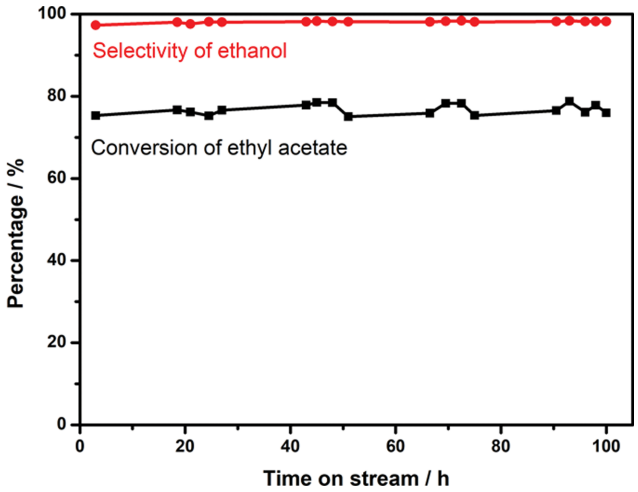

Fig. 8. The stability experiment of Cu/SiO_2-F catalysts at condition: T=280 °C; LHSV of ethyl acetate=1 h^{-1}; n(H_2)/n(ethyl acetate with 5 wt% water)=40 (molar ration) and P=2.5 MPa.

Table 3. The growth rate of conversion due to the addition of surfactants

Temperature (°C)	Cu/SiO_2-PG (%)	Cu/SiO_2-P (%)	Cu/SiO_2-C (%)	Cu/SiO_2-F (%)
220	30.4	−1.9	3.0	50.2
240	24.6	26.6	86.6	89.4
260	30.0	53.1	149.1	174.2
280	67.8	97.1	178.1	195.6

Growth rate of conversion=(Conversion$_{Cu/SiO2}$-S-Conversion$_{Cu/SiO2}$)/Conversion$_{Cu/SiO2}$*100%, S=P, PG, C and F.

assess roughly two types of Cu^{2+} content and the results is showed in Table 2. Specifically, the values of $Cu_1^{2+}/(Cu_1^{2+}+Cu_2^{2+})$ are 26.6%, 43.0%, 28.7%, 14.4% and 26.2% for Cu/SiO_2, Cu/SiO_2-C, Cu/SiO_2-F, Cu/SiO_2-PG and Cu/SiO_2-P catalysts, respectively, suggesting the addition of different surfactants has a different effect on the interactions between Cu and SiO_2.

In order to explore the influence of surfactants on catalytic performance of ethyl acetate containing water to ethanol, the prepared Cu/SiO_2 catalysts were evaluated, as shown in Fig. 7 and Fig. 8. The ethyl acetate conversion (Fig. 7) increases and ethanol selectivity (Fig. S2) decreases with the raised of reaction temperature. Meanwhile, it is clear that the catalytic performances of Cu/SiO_2 catalysts are improved due to the addition of surfactants, which are better than the conversion of Cu/SiO_2 catalyst without surfactants in the preparation process (Fig. 7). Furthermore, On the basis of Fig. 7, the growth rate of conversion was calculated and the result was showed in Table 3. From Table 3, it is found that the conversion of Cu/SiO_2-S (S=P, PG, C and F) catalysts increased 60% to 200% in comparison with that of Cu/SiO_2 catalyst at reaction temperature of 280 °C. Thereinto, Cu/SiO_2-F catalyst shows the best hydrogenation performance. Therefore, the stability experiment is performed for Cu/SiO_2-F catalyst, as shown in Fig. 8. Cu/SiO_2-F catalyst keeps 100 h without any deactivation, showing a good hydrogenation performance and water-tolertant ability.

On the basis of characterization results, the relationships between physicochemical property and catalytic performance were studied. The addition of surfactants improves the physicochemical property of Cu/SiO_2 catalysts (Table 1). However, the high copper dispersion (45.8%), small particles size (2.2 nm) and big S_{BET} (253.7 $m^2 \cdot g^{-1}$) for Cu/SiO_2-C catalyst do not cause the optimal hydrogenation performance. The order of hydrogenation performance followed Cu/SiO_2<Cu/SiO_2-PG<Cu/SiO_2-P<Cu/SiO_2-C<Cu/SiO_2-F (Table 3), while the order of copper dispersion followed Cu/SiO_2<Cu/SiO_2-PG<Cu/SiO_2-P<Cu/SiO_2-F<Cu/SiO_2-C (Table 1). Therefore, the copper dispersion had a big influence on catalytic performance. The high copper dispersion means that more active sites can be exposed in the reaction at condition containing water, which can remedy the hydrogenation performance by eliminating the negative effect that priority adsorption of water. Compared with the hydrogenation performance of Cu/SiO_2-F and Cu/SiO_2-C, the effect factor of hydrogenation performance is not only copper dispersion. The addition of surfactants not only improves D_{Cu} of Cu/SiO_2 catalysts, but also produces pores with different D_a and V_p. The published had confirmed that the preferential adsorption of water was the main reason for the deactivation [7]. Therefore, spatial restriction and the size of pore diameter also have a great effect on the hydrogenation performance at condition containing water [34]. The appropriate spatial restriction can provide many chances for ethyl acetate to touch active sites and the befitting size of pore diameter is easy to release water, so that the negative effect that priority adsorption of water further is removed. The Cu/SiO_2-F catalyst possesses optimal physicochemical property (D_{Cu} and D_a), showing good hydrogenation performance.

In order to analyse the phase change of the prepared catalysts after reaction, XRD and FT-IR are performed, and the results are shown in Fig. 9. From Fig. 9(a), all catalysts shows the diffraction

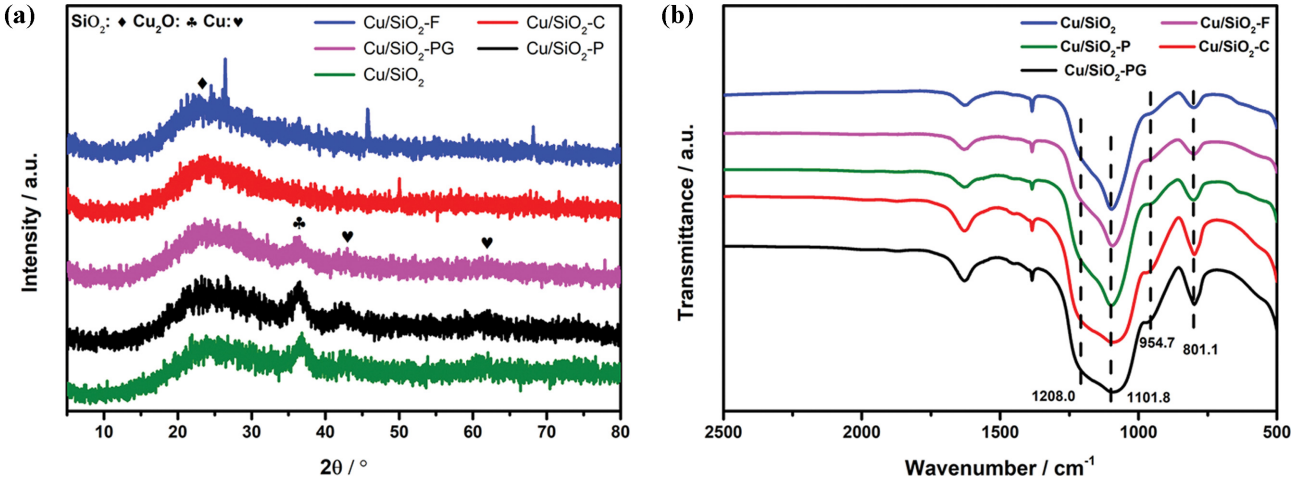

Fig. 9. (a) XRD and (b) FT-IR spectra of the prepared catalysts after reaction.

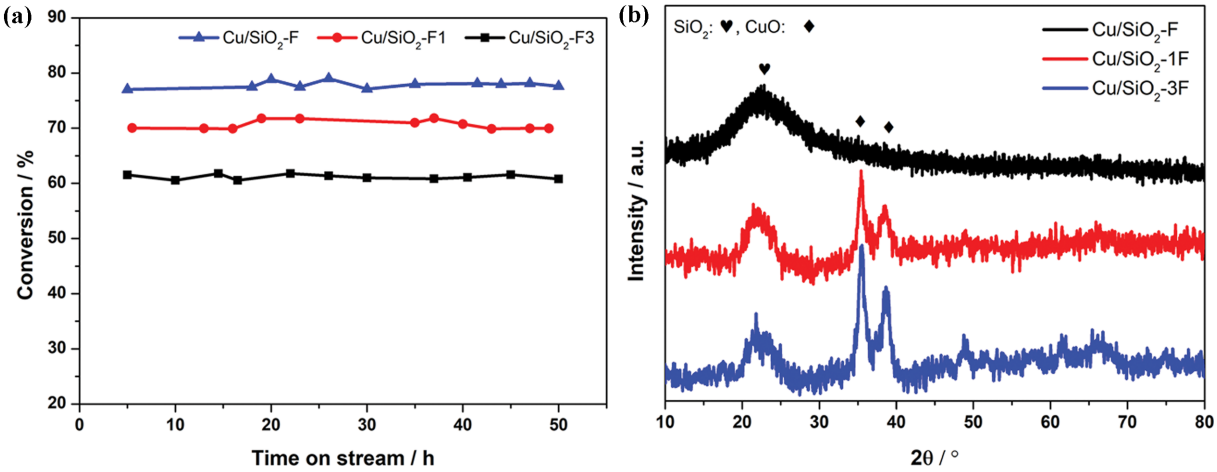

Fig. 10. (a) The conversion of a series of Cu/SiO_2-F catalysts and (b) XRD spectra of a series of Cu/SiO_2-F catalysts before reaction.

peak of SiO_2 at 22°, which is agreement with the result of Fig. 1. Meanwhile, the diffraction peaks of Cu and Cu_2O are also observed for Cu/SiO_2, Cu/SiO_2-PG and Cu/SiO_2-P catalysts. Specifically, 43.3° and 74.1° are assigned to the (1 1 1) and (2 2 0) crystal face of metal copper (PDF#04-0836). The (1 1 1) crystal face of Cu_2O is found from 36.4° (PDF#05-0667). However, there is no any diffraction peak of copper species observed for Cu/SiO_2-C and Cu/SiO_2-F catalysts, and impure peaks come from other SiO_2 that are introduced at the process of catalyst evaluation. Furthermore, the diffraction peaks intensity of copper species is low or none, suggesting than copper species are also evenly distributed on SiO_2 supports after reaction [34].

The FT-IR spectra of prepared catalysts after reaction are shown in Fig. 9(b). From Fig. 9(b), the δ_{OH} band and the ν_{SiO} of copper phyllosilicate disappeared, suggesting the phase copper phyllosilicate has been broken after reduction. The ν_{SiO} asymmetric stretching and asymmetric band of silica can also be found at 801.1 and 1,101.8 cm^{-1}. Furthermore, new weak vibrating peaks at 954.7 and 1,208.0 cm^{-1} are observed for all catalysts after reaction, which can be marked to surface Si-O- groups and asymmetric Si-O stretching, respectively. This phenomenon indicates the polycondensation degree of SiO_2 increase after reaction [35].

In order to explore the effect of surfactant amount on the hydrogenation performance of ethyl acetate containing water, the Cu/SiO_2-F, Cu/SiO_2-F1 and Cu/SiO_2-F3 catalysts were evaluated and the result was shown in Fig. 10(a). Form Fig. 10(a), it is clear that the conversion decreases with the addition amount of F127. Specifically, the conversion of ethyl acetate containing water decreases from 78% (Cu/SiO_2-F) to 63% (Cu/SiO_2-F3), showing the overmuch addition of F127 is adverse to hydrogenation performance. Fig. 10(b) shows XRD spectra of Cu/SiO_2-F, Cu/SiO_2-F1 and Cu/SiO_2-F3 catalysts before reaction. From Fig. 10(b), the diffraction peak intensity of CuO increases with the increment of the addition amount of F127, suggesting that the particle size of CuO grows up. This may be because the long chain structure of F127 accelerates the deposition and polymerization of copper particles on the surface of SiO_2, resulting in the increased of particle size. Therefore, it is referred that reason for the decline in conversion is mainly the growth of particle size, which lead to the reduction of the active sites, indicating that the exceed addition of surfactant is bad for hydrogenation performance.

In conclusion, this work studied the effect of the addition of surfactants on physicochemical property of Cu/SiO_2 catalysts, and its application in hydrogenation of ethyl acetate containing water. The characterization and hydrogenation results had demonstrated that the addition of surfactants could effectively improve the average pore diameter, specific surface area, copper dispersion and particle size and so on, which further influence hydrogenation of ethyl acetate containing water. However, the exceed addition of surfactant is bad for hydrogenation performance due to the growth of particle size. In our study, Cu/SiO_2-F catalyst, that the F127 was added in the catalyst preparation process, showed the best hydrogenation performance at condition containing water. This work provided a clear aim for researcher to develop water-tolerant Cu/SiO_2 catalysts, so that which it could meet the demand for industrial production.

ACKNOWLEDGEMENTS

This work was supported by Natural Science Foundation of Shandong Province (ZR2020QB049 and ZR2020MB030) and the Joint Fund of the Yulin University and the Dalian National Laboratory for Clean Energy (YLU-DNL Fund 2021005).

ASSOCIATED CONTENT

The detail information of characterization was given in supporting information.

NOTES

The authors declare no competing financial interest.

SUPPORTING INFORMATION

Additional information as noted in the text. This information is

available via the Internet at http://www.springer.com/chemistry/journal/11814.

REFERENCES

1. H. Zabed, J. N. Sahu, A. Suely, A. N. Boyce and G. Faruq, *Renew. Sust. Energ. Rev.*, **71**, 475 (2017).
2. Q. H. Wei, G. H. Yang, X. H. Gao, L. Tan, P. P. Ai, P. P. Zhang, P. Lu, Y. Yoneyama and N. Tsubaki, *Chem. Eng. J.*, **316**, 832 (2017).
3. Y. Wang, J. Y. Liao, J. Zhang, S. P. Wang, Y. J. Zhao and X. B. Ma, *AIChE J.*, **63**(7), 2839 (2017).
4. Y. Wang, Y. L. Shen, Y. J. Zhao, J. Lv, S. P. Wang and X. B. Ma, *ACS Catal.*, **5**(10), 6200 (2015).
5. S. H. Zhu, X. Q. Gao, Y. L. Zhu, W. B. Fan, J. G. Wang and Y. W. Li, *Catal. Sci. Technol.*, **5**(2), 1169 (2015).
6. Z. Chen, G. Zhu, Y. Wu, J. Sun, M. Abbas, P. Wang and J. Chen, *ChemistrySelect*, **4**(48), 14063 (2019).
7. Z. Chen, H. Ge, P. Wang, J. Sun, M. Abbas and J. Chen, *Mol. Catal.*, **488**, 110919 (2020).
8. J. Z. Zheng, X. Duan, H. Lin, Z. Gu, H. Fang, J. Li and Y. Yuan, *Nanoscale*, **8**(11), 5959 (2016).
9. W. Wang, M. Ding, L. Ma, X. Yang, J. Li, N. Tsubaki, G. Yang, T. Wang and X. Li, *Fuel*, **164**, 347 (2016).
10. W. Liu, J. Qi, P. Bai, W. Zhang and L. Xu, *Appl. Catal. B-Environ.*, **272**, 118974 (2020).
11. H. R. Yue, Y. J. Zhao, S. Zhao, B. Wang, X. B. Ma and J. L. Gong, *Nat. Commun.*, **4**, 7 (2013).
12. H. Jiang, D. Kong, Y. Niu and S. Wang, *Catal. Sci. Technol.*, **10**(23), 8086 (2020).
13. M. M. Ma, X. Y. Zhao, X. T. Wang, F. F. Gong, F. L. Yuan, Z. B. Li and Y. J. Zhu, *Catal. Commun.*, **133**, 5 (2020).
14. P. Zhang, X. Peng, Y. Araki, Y. Fang, Y. Zeng, R. Kosol, G. Yang and N. Tsubaki, *Catal. Sci. Technol.*, **10**(24), 8410 (2020).
15. L. Li, D. Mao, J. Yu and X. Guo, *J. Power Sources*, **279**, 394 (2015).
16. Q. Q. Wang, J. X. Chen, H. Zhang, W. W. Wu, Z. Q. Zhang and S. J. Dong, *Nanoscale*, **10**(40), 19140 (2018).
17. S. J. Chen, G. S. Zhang, Y. J. Li, J. L. Li, R. J. Lv, P. Wang, N. Chen, X. Chen, Y. Y. Huang, L. Yang and D. C. Zhao, *J. Nanosci. Nanotechnol.*, **20**(9), 5636 (2020).
18. H. R. Mahmoud, S. A. El-Molla and M. M. Ibrahim, *Renew. Energ.*, **160**, 42 (2020).
19. F. C. F. Marcos, L. Lin, L. E. Betancourt, S. D. Senanayake, J. A. Rodriguez, J. M. Assaf, R. Giudici and E. M. Assaf, *J. CO_2 Util.*, **41**, 101215 (2020).
20. S. Karimi, F. Meshkani, M. Rezaei and A. Rastegarpanah, *Fuel*, **284** (2021).
21. K. Tripathi, R. Singh and K. K. Pant, *Top. Catal.*, **64**, 395 (2021).
22. C. J. G. Van Der Grift, A. F. H. Wielers, B. P. J. Jogh, J. Van Beunum, M. De Boer, M. Versluijs-Helder and J. W. Geus, *J. Catal.*, **131**(1), 178 (1991).
23. Z. Yuan, L. Wang, J. Wang, S. Xia, P. Chen, Z. Hou and X. Zheng, *Appl. Catal. B-Environ.*, **101**(3), 431 (2011).
24. K. Sing, D. H. Everett, R. A. W. Haul, L. Moscou, R. A. Pierotti, J. Rouquerol and T. Siemieniewska, *Pure Appl. Chem.*, **57**, 603 (1985).
25. M. Donohue and G. L. Aranovich, *Adv. Colloid Interface*, **76**, 137 (1998).
26. L. F. Chen, P. J. Guo, M. H. Qiao, S. R. Yan, H. X. Li, W. Shen, H. L. Xu, and K. N. Fan, *J. Catal.*, **257**(1), 172 (2008).
27. W. Di, J. H. Cheng, S. X. Tian, J. Li, J. Y. Chen and Q. Sun, *Appl. Catal. A-Gen.*, **510**, 244 (2016).
28. T. Toupance, M. Kermarec, J.-F. Lambert and C. Louis, *J. Phy. Chem. B*, **106**(9), 2277 (2002).
29. Z. W. Huang, F. Cui, H. X. Kang, J. Chen, X. Z. Zhang and C. G. Xia, *Chem. Mat.*, **20**(15), 5090 (2008).
30. Y. F. Zhu, X. Kong, X. Q. Li, G. Q. Ding, Y. L. Zhu and Y. W. Li, *ACS Catal.*, **4**(10), 3612 (2014).
31. Y. T. Liu, J. Ding, J. Q. Sun, J. Zhang, J. C. Bi, K. F. Liu, F. H. Kong, H. C. Xiao, Y. P. Sun and J. G. Chen, *Chem. Commun.*, **52**(28), 5030 (2016).
32. Z. Huang, F. Cui, H. Kang, J. Chen, X. Zhang and C. Xia, *Chem. Mat.*, **20**(15), 5090 (2008).
33. I. Platzman, R. Brener, H. Haick and R. Tannenbaum, *J. Phy. Chem. C*, **112**(4), 1101 (2008).
34. Z. Chen, T. Zhang, X. Zhao, X. L. Zhang, D. Wang and S. Wei, *ChemistrySelect*, **6**(47), 13479 (2021).
35. Z. Chen, J. Zhang, M. Abbas, Y. Xue, J. Sun, K. Liu and J. Chen, *Ind. Eng. Chem. Res.*, **56**(33), 9285 (2017).

Supporting Information

The improvement effect of surfactants on hydrogenation at condition containing water for Cu/SiO_2 catalysts

Zheng Chen*,†, Xueying Zhao*, Shuwei Wei*, Dengfeng Wang*, Xuelan Zhang*, and Jianfeng Shan*,,†**

*College of Chemistry, Chemical Engineering and Materials Science, Zaozhuang University, Zaozhuang 277160, Shandong, China
**College of Chemistry and Chemical Engineering, Xinyang Normal University, Xinyang 464000, China
(*Received 16 February 2022 • Revised 21 May 2022 • Accepted 25 June 2022*)

1. Characterization

The powder X-ray diffraction (XRD) pattern of the prepared catalysts was recorded on a Shimadzu XRD-6000 diffractometer using Cu Kα radiation (λ=1.5418 Å) in the 2θ scanning range between 10° and 80°. The dispersion and specific surface area of Cu^0 (D^0_{Cu} and S^0_{Cu}) were measured by N_2O oxidation at 50 °C. The more details could be found from the below. Fourier transform infrared (FT-IR) spectra was performed in transmission mode from 2,500-500 cm^{-1} using a Bruker Vector 22 spectrometer equipped with a DTGS detector and a KBr beam splitter. The specific surface area was determined by BET (Brunauer-Emmett-Teller) measurements using a Tristar II3020 N2 adsorption analyzer. Then, the TPR experiments were performed as follows: the fresh catalysts (20 mg) were placed in a quartz reactor and were reduced by a 5% H_2/N_2 gas mixture with a flow rate of 50 ml min^{-1}, ramping at 10 °C min^{-1} to the final temperature. X-ray photoelectron spectroscopy (XPS, AXIS ULTRA DLD) was carried out to analyze the elemental valence of the surface. Meanwhile, hydrogen consumption was recorded using a thermal conductivity detector (TCD). The morphology of the samples was characterized by means of a high-resolution transmission electron microscope (HRTEM, JEM 2100F).

N_2O-H_2 Redox Titration Procedure

The number of surface metallic copper sites was determined by dissociative N_2O adsorption at 50 °C [1,2]. Catalysts were first reduced by a 5% H_2/N_2 gas mixture with a flow rate of 50 ml min^{-1}, ramping at 5 °C min^{-1} to 300 °C for 10 min. The amount of hydrogen consumption in first TPR (TPR1) was denoted as X. And then, the catalyst bed was purged with Ar and cooled to 50 °C. Surface copper atoms were oxidized in a N_2O (50 mL/min) at 50 °C for 0.5 h. Finally, samples were flushed with 5% H_2/N_2 to remove the oxidant for 1 h and then to start another TPR run. Hydrogen consumption in the second TPR (TPR2) was denoted as Y.

The dispersion of Cu and exposed Cu surface area are calculated on the equations reported by Van Der Grift et al. [1]

All copper atoms were reduced in the first TPR:

$CuO+H_2 \rightarrow Cu+H_2O$, hydrogen consumption=X

Surface copper atoms that were oxidized to Cu_2O by N_2O at 50 °C were reduced in the second TPR:

$Cu_2O+H_2 \rightarrow 2Cu+H_2O$, hydrogen consumption=Y

And the dispersion of Cu and exposed Cu surface area were calculated as:

$D=(2\ Y/X)\times 100\%$; $S=1353\times Y/X$ (m^2_{Cu}/g_{Cu}); $d_{v.s.}=0.5\ X/Y$ (nm)

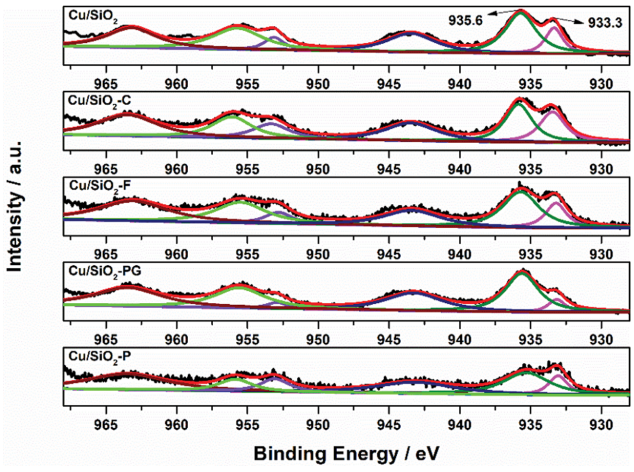

Fig. S1. The XPS of the prepared catalysts.

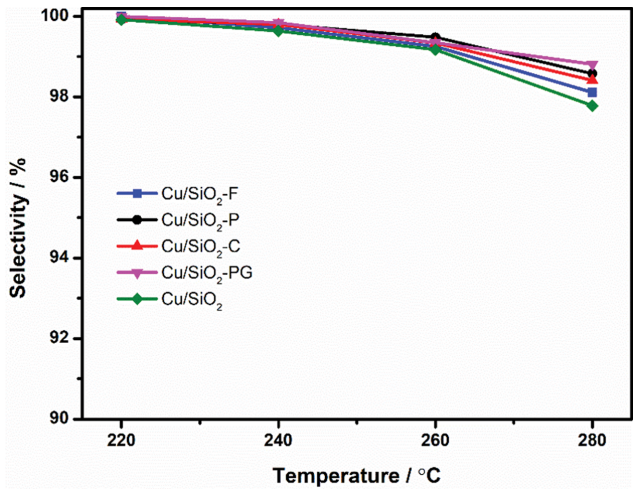

Fig. S2. The selectivity of ethanol for the prepared catalysts at condition: T=220, 240, 260 and 280 °C; LHSV of ethyl acetate= 1 h^{-1}; n(H_2)/n(ethyl acetate with 5 wt% water)=40 (molar ration) and P=2.5 MPa.

REFERENCE

1. C. J. G. van der Grift, A. F. H. Wielers, B. P. J. Jogh, J. van Beunum, M. de Boer, M. Versluijs-Helder and J. W. J. Geus, *J. Catal.*, **131**, 178 (1991).